

## Journal of Thermal Engineering

Web page info: https://jten.yildiz.edu.tr DOI: 10.14744/thermal.0001001



## **Research Article**

# Mathematical simulation of magnetohydrodynamic slip transportation phenomena towards non-linear stretching cylinder induced with free stream velocity utilizing buongiorno's model

Saloni GUPTA<sup>1,\*</sup>, Chinta Mani TIWARI<sup>1</sup>

<sup>1</sup>Maharishi School of Science, Maharishi University of Information Technology, Lucknow, 226013, India

## **ARTICLE INFO**

Article history

Received: 31 December 2024 Accepted: 10 April 2025

#### **Keywords:**

Brownian Motion; Heat Radiation; MHD; Non-linear Stretching Cylinder; Partial Slip; Thermophoresis

#### **ABSTRACT**

The manuscript's goal is to examine how magneto-hydrodynamic slip flow affects a non-linear stretching cylinder while producing heat and radiation in presence of free stream velocity. Non-linear behavior produces a flow along with Brownian motion and thermophoresis. The shooting technique model was employed to solve moulded equations numerically following the advent of the Runga Kutta Fehlberg approach in MATLAB programming. The attractive pattern combined thermophoresis with a study of the effects of Brownian motion are also discussed. The effects of important fluid characteristics, such as outer velocity, heat radiation, and velocity of slip, thermophoresis, and Brownian motion are studied and represented via graphs and tables. It is revealed that, heat transfer rate falls down by 71.31% with increment in free stream velocity whereas heat transfer rate rises up by 34.43% with rise in Brownian motion parameter. Moreover, skin friction coefficient intensifies with increment in free stream velocity parameter. Current research has major applications in the production of glass fibers, biotechnological field, encompassing power plants, manufacturing of tetra packs, refrigeration systems, medical science, micro-electro-mechanical Systems and in wide variety of industries.

Cite this article as: Gupta S, Tiwari CM. Mathematical simulation of magnetohydrodynamic slip transportation phenomena towards non-linear stretching cylinder induced with free stream velocity utilizing buongiorno's model. J Ther Eng 2025;11(6):1618–1626.

## **INTRODUCTION**

In many industrial applications that depends on understanding the mechanisms of different types of energy transfer occurring within the system. The flow towards a stretching sheet was examined by Crane [1]. By taking into consideration a thin metal stretching sheet, the comparison between experimental and theoretical results has been displayed by Yoon et al. [2]. Sarma and Rao [3] presented the viscoelastic behavior of fluid flow. Manjunatha et al. [4] also investigated the heat source & radiation effects in porous medium. These days, a lot of scientist are concentrating on MHD non-Newtonian nano-fluids because of their many uses in fields like engineering, biological materials, photodynamic therapy, and food processing. Nano-fluid is the general term for a fluid that contains nanoparticles

This paper was recommended for publication in revised form by Editor-in-Chief Ahmet Selim Dalkılıç



<sup>\*</sup>Corresponding author.

<sup>\*</sup>E-mail address: saloni.20.jindal@gmail.com

(sizes between 1 and 100 nanometers), according to Choi [5]. Additionally, the prospective uses of nanofluids in drug delivery and biomedical imaging have been investigated. To completely comprehend the features and transport capabilities of nanofluids as well as their potential for practical uses, more study is necessary. Before nanofluids are extensively used, concerns regarding the safety and potential effects of nanoparticles on the environment must be thoroughly examined. In the fields of pharmaceuticals, electronics, refrigerators and other household appliances, and power and chemical engineering, nanofluids have unique qualities and characteristics. Afterthat, Convection in nanofluid was described by Buogiorno [6]. Many scientists have studied the transport phenomenon of many Newtonian or non-Newtonian fluid models [7-11].

Magnetohydrodynamics, or MHD for short, is the study of how electrically conducting liquids behaves in presence of magnetism. It analyses how electrically charged particles and magnetic fields interact within a fluid by combining concepts from fluid dynamics and electromagnetism. Studies in the field of magnetohydrodynamics are frequently focused on plasmas, which are states of matter made up of charged particles (ions and electrons) that are capable of electrical conduction. This field includes a wide range of research questions, such as studying plasma dynamics in fusion reactors, studying solar flares and steroidal projectiles, and delving into the mechanisms underlying Earth's magnetosphere. Hayat et al. [12] provided an interpretation of the Powell-Eyring MHD nanofluid flow. The flow conveyance on a non-linear stretched sheet with suction/injection was researched by Siddheshwar and Mahabaleshwar [13]. Researchers have also looked at non-linear influence towards stretched surfaces in a variety of real-world scenarios [14-19]. Recently, impact of MHD nanofluid with existence of slip conditions is revealed by [20]. Akaje et al. [21] studied the transport phenomenon induced by inclined surface in presence of MHD Casson nanofluid. Bolarin et al. [22] discussed the nanofluid boundary layer fluid flow induced by inclined surface. Influence of two phase transport phenomenon in presence of magnetic field induced by resolving system analytically has been investigated by Gholinia et al. [23]. Rana et al. [24] discussed the influence of Ag-MgO (50: 50)/water based hybrid nanofluid utilizing neural network by following FEM simulation. Free convection MHD energy transformation has been studied by Rana et al. [25] in presence of hybrid nanofluids. In recent years, influence of MHD under different boundary conditions has been studied by researchers in [26-31].

Investigations on combined influence of MHD slip flow, outer velocity, heat radiation & generation on non-linear stretching cylinders have not yet shown any results. To fill this gap, impact of free stream velocity with slip conditions and thermal radiation over non-linear surface has been studied out in this research. Mainly the quantitative results gives a new hike to this research to make novel one and has major applications in the biotechnological field,

encompassing power plants, refrigeration systems, medical science, micro-electro-mechanical Systems and in wide variety of industries. The following list indicates this paper's main goal. To establish the mathematical equations that relate to the problem and the equivalent boundary conditions, such as continuity, momentum, energy, and concentration. Using the appropriate non-dimensional parameters and variables, dimensional O.D.E's are converted into dimensionless P.D.E's. Major objectives of the study are:

- To obtain the numerical solutions, MATLAB 2014a will be used in conjunction with the Runge Kutta Fehlberg approach.
- To investigate the effects of incidental features on skin friction, temperature, concentration, velocity, Nusselt and Sherwood number.
- To examine the combined effects of heat radiation and heat generation on temperature and velocity profiles, together with plots and tables.
- To illustrate the contrast between the impact of radiation and thermoelectric power on nanofluids.

#### **MATERIALS AND METHODS**

In current study, 2-D incompressible slip flow in MHD nanofluid towards non-linear stretched surface has been induced. Non-linear behavior produces a flow along with Brownian motion and thermophoresis with considered stretching velocity  $U_w = cx^n/L$ , where c is a constant, n represents non-linear stretching parameter and L represents characteristic length. Two component Buogiorno's [6] model has been followed in current study & Magnetic field is assumed to be applied in radial direction. The physical representation of the current issue is shown in Figure 1. Here, R is the radius of the cylinder. In terms of Cartesian coordinates, the fundamental governing equations for nanofluid are defined as follows [32, 33]:

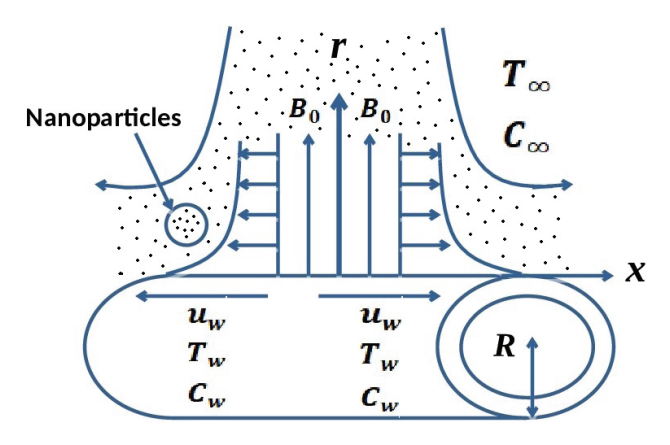


Figure 1. Physical model of the problem.

$$\frac{\partial}{\partial x}(ru) + \frac{\partial}{\partial r}(rv) = 0, \tag{1}$$

$$u\frac{\partial u}{\partial x} + v\frac{\partial u}{\partial r} = v\left(\frac{\partial^2 u}{\partial r^2} + \frac{1}{r}\frac{\partial u}{\partial r}\right) - \frac{\sigma B_0^2}{\rho}(u - U) + U\frac{\partial U}{\partial x}, \quad (2)$$

$$u\frac{\partial T}{\partial x} + v\frac{\partial T}{\partial r} = \tau \left[ D_B \frac{\partial C}{\partial r} \frac{\partial T}{\partial r} + \frac{D_T}{T_\infty} \left( \frac{\partial T}{\partial r} \right)^2 \right]$$

$$+ \alpha \left( \frac{\partial^2 T}{\partial r^2} + \frac{1}{r} \frac{\partial T}{\partial r} \right) \frac{1}{(\rho c)_f} \frac{1}{r} \frac{\partial}{\partial r} (rq_r)$$

$$+ \frac{Q_0}{(\rho c)_f} (T - T_\infty)$$
(3)

$$u\frac{\partial C}{\partial x} + v\frac{\partial C}{\partial r} = D_B \left( \frac{\partial^2 C}{\partial r^2} + \frac{1}{r} \frac{\partial C}{\partial r} \right) + \frac{D_T}{T_\infty} \left( \frac{\partial^2 T}{\partial r^2} + \frac{1}{r} \frac{\partial T}{\partial r} \right), \quad (4)$$

The flow model is described by boundary conditions as follows:

$$u = eu_w(x) + N\mu\left(\frac{\partial u}{\partial r}\right), v = 0, T = T_w, C = C_w \text{ at } r = R,$$

$$u \to U = \frac{bx}{I}, T \to T_\infty, C \to C_\infty \text{ as } r \to \infty$$
(5)

Where  $N\mu$  the velocity is slip factor and e is the stretching velocity parameter.

Using similarity variables

$$\xi = \frac{r^2 - R^2}{2R} \left(\frac{c}{vL}\right)^{\frac{1}{2}}, \ \psi = \left(\frac{vc}{L}\right)^{\frac{1}{2}} xRf_{\delta}(\xi),$$

$$\theta_{\delta}(\xi) = \frac{T - T_{\infty}}{T_{\delta} - T_{\infty}} \text{ and } \phi_{\delta}(\xi) = \frac{C - C_{\infty}}{C_{w} - C_{\infty}}$$
(6)

After substituting (6) into (2)-(4), we obtain

$$(1+2\xi\gamma)\left(1+\frac{4}{3}Rd\right)\theta_{\delta}" + \left[2\gamma\left(1+\frac{4}{3}Rd\right) + Pr\left(\frac{n+1}{2}\right)f_{\delta}\right]\theta_{\delta}'$$

$$+ Pr\left[Nb\left(1+2\xi\gamma\right)\theta_{\delta}'\phi_{\delta}' + Nt\left(1+2\xi\gamma\right)\theta_{\delta}'^{2} + Q\theta_{\delta}\right] = 0$$

$$(8)$$

$$\left(1+2\xi\gamma\right)\phi_{\delta}"+\left(\frac{n+1}{2}\right)Sc_{f_{\delta}}\phi_{\delta}"+2\gamma\phi_{\delta}"+\left(1+2\xi\gamma\right)\frac{Nt}{Nb}\theta_{\delta}"+2\gamma\frac{Nt}{Nb}\theta_{\delta}"=0 \tag{9}$$

Transformed (5) which become,

$$f_{\delta}(0) = 0, \ f_{\delta}'(0) = e + df_{\delta}''(0), \ \theta_{\delta}(0) = 1, \ \phi_{\delta}(0) = 1,$$
  
$$f_{\delta}'(\xi) \to \lambda, \ \theta_{\delta}(\xi) \to 0, \ \phi_{\delta}(\xi) \to 0 \text{ as } \xi \to \infty$$
 (10)

Later, the velocity slip parameter *d* is defined as

$$d = N\mu \frac{r}{R} \left(\frac{c}{\nu L}\right)^{\frac{1}{2}} = N_0 \left(\frac{c}{\nu L}\right)^{\frac{1}{2}} \tag{11}$$

where  $N = N_0 R / \mu r$ ,  $N_0$  being the constant wall slip velocity.

Dimensionless parameters; free stream velocity, Prandtl number, Brownian motion, thermophoresis, heat generation, heat radiation and magnetic parameters are symbolically given by

$$\lambda = \frac{b}{c}, Pr = \frac{v}{\alpha}, Sc = \frac{v}{D_B}, Nb = \frac{\left(\rho c\right)_p D_B \left(C_w - C_\infty\right)}{\left(\rho c\right)_f v},$$

$$Nt = \frac{\left(\rho c\right)_p D_T \left(T_f - T_\infty\right)}{\left(\rho c\right)_f T_\infty v} \quad Q = \frac{Q_0 L}{c\left(\rho c\right)_f}, Rd = \frac{4\sigma^* T_\infty^3}{kk^*}, \quad (12)$$

$$M = \frac{\sigma B_0^2 L}{\rho c}$$

 $Sh_x$ ,  $Nu_x$  and  $C_f$  are defined as:

$$Sh_{x} = \frac{xq_{m}}{D_{B}\left(C_{w} - C_{\infty}\right)}, Nu_{x} = \frac{xq_{w}}{k\left(T_{f} - T_{\infty}\right)}, C_{f} = \frac{\tau_{w}}{\rho U_{\infty}^{2}}$$
(13)

where  $q_m$ ,  $q_w$  and  $\tau_w$  are as follows,

$$q_{m} = -D_{B} \left( \frac{\partial T}{\partial r} \right)_{r=R}, \quad q_{w} = -\left( \alpha + \frac{16\sigma * T_{\infty}^{3}}{3(\rho c)_{f} k *} \right) \left( \frac{\partial T}{\partial r} \right)_{r=R},$$

$$\tau_{w} = \mu \left( \frac{\partial u}{\partial r} \right)_{r=R}$$
(14)

with k and m are the thermal conductivity and dynamic viscosity of the nanofluid serially. Using the similarity variables eq (6), eq (13) becomes

$$Sh_{x}Re_{x}^{-1/2} = -\phi_{\delta}'(0), \quad Nu_{x}Re_{x}^{-1/2} = -\left(1 + \frac{4}{3}Rd\right)\theta_{\delta}'(0),$$

$$C_{f}Re_{x}^{1/2} = f_{\delta}"(0)$$
(15)

where  $Re_x = U_{\infty}x/\nu$  is the local Reynolds number.

### **Numerical Solution**

Due to their highly non-linear behavior, D.E's (7)–(9) cannot be solved analytically. Our method of choice for solving D.E's (7)–(9) along with B.C's (10) is the numerical procedure known as the RKF approach. Shooting technique has been adopted to solve the system of equation and the process has been displayed via figure 2 using flow chart. The following is a rearrangement of the controlling non-linear ordinary differential equations:

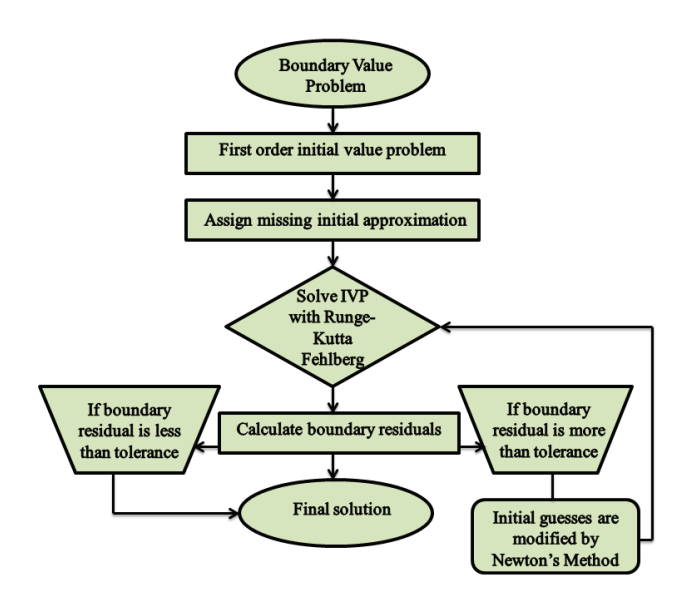


Figure 2. Flow chart of shooting technique.

$$f_{\delta}^{""} = \frac{-1}{\left(1 + 2\zeta \gamma\right)} \left[ 2\gamma f_{\delta}^{"} + \left(\frac{n+1}{2}\right) f_{\delta} f_{\delta}^{"} - n f_{\delta}^{'2} - M \left(f_{\delta}^{'} - \lambda\right) + n\lambda^{2} \right]$$
(16)

$$\theta_{\delta}" = \frac{-1}{\left(1 + 2\zeta\gamma\right)\left(1 + \frac{4}{3}Rd\right)} \begin{bmatrix} \left\{2\gamma\left(1 + \frac{4}{3}Rd\right) + Pr\left(\frac{n+1}{2}\right)f_{\delta}\right\}\theta_{\delta}' \\ + Pr\left\{Nb\left(1 + 2\zeta\gamma\right)\theta_{\delta}'\phi_{\delta}' \\ + Nt\left(1 + 2\zeta\gamma\right)\theta_{\delta}'^{2} + Q\theta_{\delta}\right\} \end{bmatrix}$$
(17) Where,

$$\phi_{\delta}^{"} = \frac{-1}{\left(1 + 2\xi\gamma\right)} \left[ \left(\frac{n+1}{2}\right) Scf_{\delta}\phi_{\delta}' + 2\gamma\phi_{\delta}' + \left(1 + 2\xi\gamma\right) \frac{Nt}{Nb} \theta_{\delta}'' + 2\gamma \frac{Nt}{Nb} \theta_{\delta}' \right]$$
(18)

Transformed 1st order D.E's are:

$$S_1 = S_2 \tag{19}$$

$$S_2' = S_3 \tag{20}$$

$$s_{3}' = \frac{-1}{\left(1 + 2\zeta\gamma\right)} \left[ 2\gamma s_{3} + \left(\frac{n+1}{2}\right) s_{1}s_{3} - ns_{2}^{2} - M\left(s_{2} - \lambda\right) + n\lambda^{2} \right]$$
 (21)

$$s_4' = s_5$$
 (22)

$$s_{5}' = \frac{-1}{\left(1 + 2\zeta\gamma\right)\left(1 + \frac{4}{3}Rd\right)} \begin{bmatrix} \left\{2\gamma\left(1 + \frac{4}{3}Rd\right) + Pr\left(\frac{n+1}{2}\right)s_{1}\right\}s_{5} \\ + Pr\left\{Nb\left(1 + 2\zeta\gamma\right)s_{5}s_{7} \\ + Nt\left(1 + 2\zeta\gamma\right)s_{5}^{2} + Qs_{4}\right\} \end{bmatrix}$$
(23)

$$S_6' = S_7 \tag{24}$$

$$s_{7}' = \frac{-1}{(1+2\xi\gamma)} \left[ \left( \frac{n+1}{2} \right) Scs_{1}s_{7} + 2\gamma s_{7} + \left( 1+2\xi\gamma \right) \frac{Nt}{Nb} s_{5}' + 2\gamma \frac{Nt}{Nb} s_{5} \right]$$
 (25)

B.C's are reduced to

$$\begin{bmatrix} S_{1} \\ S_{2} \\ S_{3} \\ S_{4} \\ S_{5} \\ S_{6} \\ S_{7} \end{bmatrix} = \begin{bmatrix} 0 \\ e + \sigma h_{1} \\ h_{1} \\ h_{2} \\ h_{2} \\ h_{3} \end{bmatrix}$$
(26)

$$f_{\delta} = s_{1}, \ f_{\delta}' = s_{2}, \ f_{\delta}'' = s_{3}, \ f_{\delta}''' = s_{3}',$$

$$\theta_{\delta} = s_{4}, \ \theta_{\delta}' = s_{5}, \ \theta_{\delta}'' = s_{5}',$$

$$\phi_{\delta} = s_{6}, \ \phi_{\delta}' = s_{7}, \ \phi_{\delta}'' = s_{7}'$$
(27)

# **Code Validation**

For determining the final results in the current study, we employ the RKF approach, and the numerical procedure we are using the shooting technique. At the border, we assume a constant temperature and concentration of nanoparticles. The boundaries' restrictions are as follows:

$$u_w = ax^n; T = T_w \text{ and } C = C_w$$
 (28)

In present problem, we compare our results for  $-\theta'_{\delta}(0)$ for different Pr and fixed n = 1, d = 0, Nt = Nb = 0 and as shown in Table 1.

**Table 1.** Comparison of for Nusselt number  $-\theta'_{\delta}(0)$ .

Pr	Gorla and Sidawi [34]	Residual Error	Mankinde and Aziz [35]	Residual Error	Present Result
2	0.9114	-0.0001	0.9114	-0.0001	0.9113
7	1.8954	0.0000	1.8954	0.0000	1.8954
20	3.3539	0.0000	-	-	3.3539
70	6.4622	-0.0001	-	-	6.4621

#### NUMERICAL RESULTS AND DISCUSSION

The current investigation determines the numerical solution for D.E's (7)-(9) when B.C's (10) are obtained using the RKF method. Determining the influence of important fluid factors namely  $\lambda$ , Rd, d, Nt and Nb on  $f'_{\delta}(0)$ ,  $\theta_{\delta}(0)$  and  $\phi_{\delta}(0)$  is the primary motivation for solving the current problem. Table 2-6 demonstrate the impact of fluid parameters  $\lambda=0.1,0.3,0.5,0.7,Nb=0.1,0.3,0.5,0.7,Nt=0.1,0.3,0.5,0.7,Rd=1,3,5,7,$  and 0, 0.2, 0.4, 0.6 on  $f''_{\delta}(0)$ ,  $-\theta'_{\delta}(0)$  and  $-\phi'_{\delta}(0)$  in current problem.

**Table 2.**  $f''_{\delta}(0)$ ,  $-\theta'_{\delta}(0)$  and  $-\phi'_{\delta}(0)$  against  $\lambda$ .

λ	$f''_{\delta}(0)$	$-\theta'_{\delta}(0)$	$-\phi'_{\delta}(0)$	
0.1	-1.01740	0.30784	1.11220	
0.3	-0.87538	0.39182	1.12607	
0.5	-0.67682	0.46528	1.16666	
0.7	-0.43353	0.52737	1.21691	

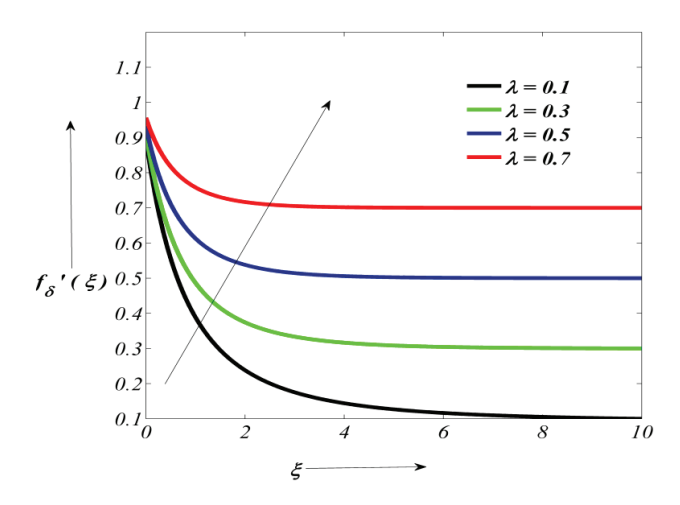


**Figure 3.** Velocity profile against  $\lambda$ .

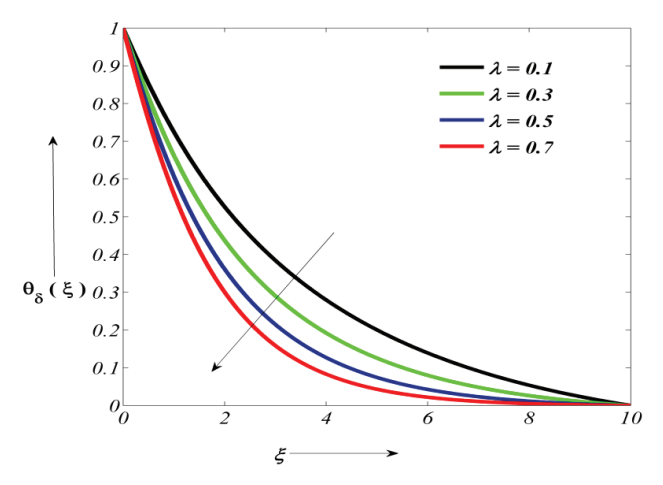


**Figure 4.** Temperature profile against  $\lambda$ .

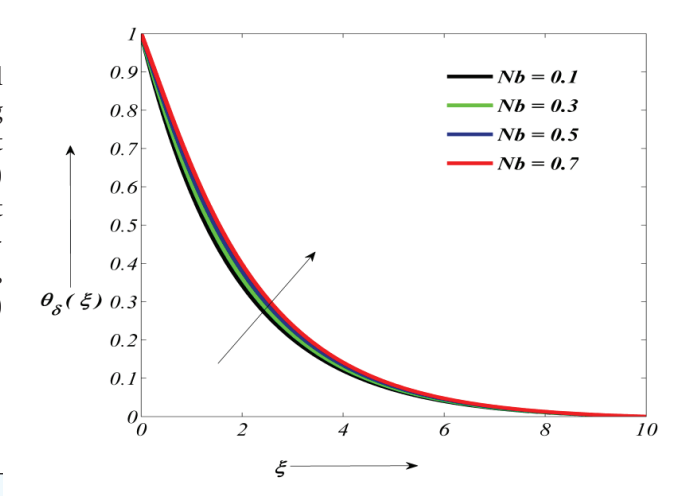


Figure 5. Temperature profile against Nb.

**Table 3.**  $f''_{\delta}(0)$ ,  $-\theta'_{\delta}(0)$  and  $-\phi'_{\delta}(0)$  against Nb.

Nb	$f''_{\delta}(0)$	$-\theta'_{\delta}(0)$	$-\phi'_{\delta}(0)$	
0.1	-0.67682	0.53271	0.99747	
0.3	-0.67682	0.46528	1.16666	
0.5	-0.67682	0.40426	1.19699	
0.7	-0.67682	0.34930	1.20765	

**Table 4.**  $f''_{\delta}(0)$ ,  $-\theta'_{\delta}(0)$  and  $-\phi'_{\delta}(0)$  against Nt.

Nt	$f''_{\delta}(0)$	$-\theta'_{\delta}(0)$	$-\phi'_{\delta}(0)$
0.1	-0.67682	0.51061	1.15897
0.3	-0.67682	0.46528	1.16666
0.5	-0.67682	0.42344	1.21242
0.7	-0.67682	0.38480	1.29061

Figures 3, and 4 displayed the impact of  $\lambda(0.1 \le \lambda \le 0.7)$ on  $f_{\delta}'(\xi)$  and  $\theta_{\delta}(\xi)$  respectively. For large  $\lambda$ , it is described that the velocity profile rises and vanished at the surface of cylinder as visualized in Figure 3. Because of this, very less declination in field temperature is noticed for various entries of that can be observed in Figure 4. Hence, local Nusselt number also rise as displayed in Table 2. Figures 5 and 6 demonstrate profile of temperature and concentration with change in value of  $Nb(0.1 \le Nb \le 0.7)$ . A random striking of poised elements is the Brownian motion that shows its existence when liquid particles strike with each another will create an arbitrary motion and that performs an increment in temperature as well as in concentration as displayed in Figures 5 and 6. Brownian motion of suspended (Pendolus) particles is the main reason for rise in kinetic energy of nano particle and due to this it enhance the thermal boundary layer thickness. Consequently, temperature gradient falls down for higher Nb (See Table 3).

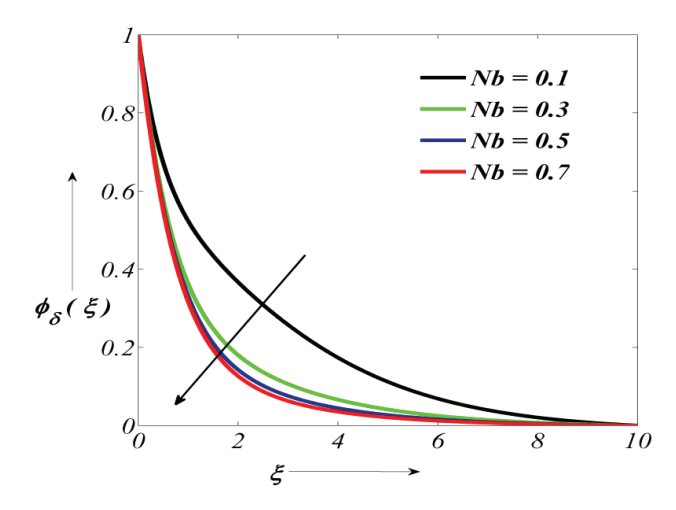


**Figure 6.** Concentration profile against Nb.

**Table 5.**  $f''_{\delta}(0)$ ,  $-\theta'_{\delta}(0)$  and  $-\phi'_{\delta}(0)$  for distinct values of fluid parameter Rd.

Rd	$f''_{\delta}(0)$	$-\theta'_{\delta}(0)$	$-\phi'_{\delta}(0)$	
1	-0.67682	0.46528	1.16666	
3	-0.67682	0.43887	1.16466	
5	-0.67682	0.42966	1.16669	
7	-0.67682	0.42559	1.16790	

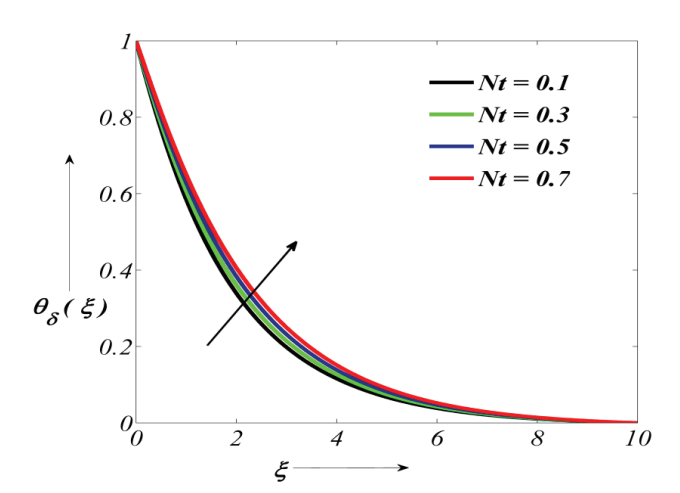


**Figure 7.** Temperature profile against *Nt*.

Little increment is seen in  $\theta_{\delta}(\xi)$  for higher Nb. For higher value of Brownian motion parameter Nb, collision between fluid particle will by which nanoparticle concentration declines. Also, concentration boundary layer thickness decreases as observed in Figure 6. Figures 7 and 8 presents the  $\theta_{\delta}(\xi)$  &  $\phi_{\delta}(\xi)$  plots affected by the thermophoresis, respectively. With augmentation in thermophoresis Nt, there is a declination in the temperature gradient, due to

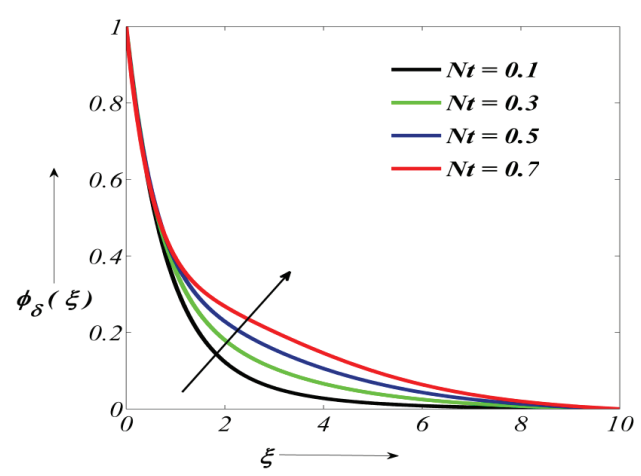
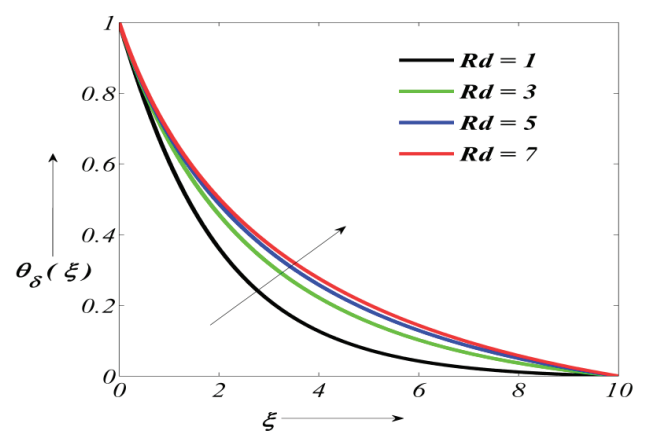
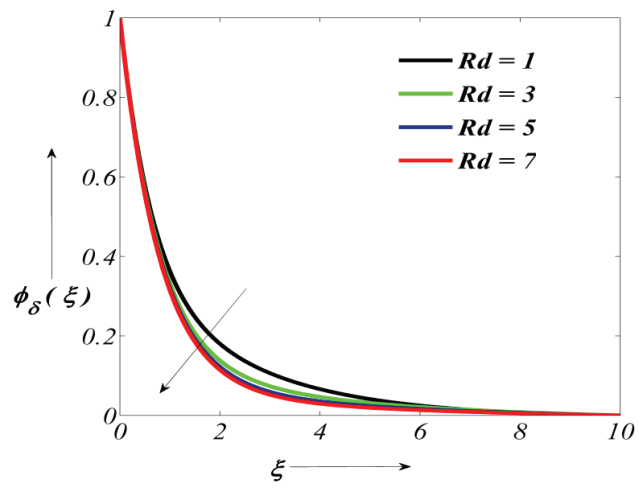


Figure 8. Concentration profile against Nt.



**Figure 9.** Temperature profile against *Rd*.



**Figure 10.** Concentration profile against *Rd*.

which nanoparticle conduction falls down. Consequently, ultrafine elements migrate from hotter to cooler zone, that simultaneously increasing the width of the boundary layer and raising the temperature. This increase in thermal boundary layer thickness causes a decrease in the Nusselt number, as observed in Table 4. Conversely, in Figures 8,  $\phi_{\delta}(\xi)$  increases and the width of the concentration boundary layer also increases with higher values of the thermophoresis parameter. Additionally, plots are distinct for 0.0  $\leq \xi \leq 8.2$  (approx) and converges with  $\xi \to \infty$ . In Figure 9, fluid temperature rises as the radiation parameter Rd increases, indicating a higher surface heat flux associated with higher Rd values. Additionally, the thermal boundary layer thickness expands with increasing Rd, suggesting a broader spread of heat transfer over the surface.

**Table 6.**  $f''_{\delta}(0)$ ,  $-\theta'_{\delta}(0)$  and  $-\phi'_{\delta}(0)$  for distinct values of fluid parameter d.

d	$f''_{\delta}(0)$	$-\theta'_{\delta}(0)$	$-\phi'_{\delta}(0)$
0.0	-0.79492	0.47739	1.18293
0.2	-0.59077	0.45608	1.15436
0.4	-0.47280	0.44288	1.13680
0.6	-0.39512	0.43377	1.12477

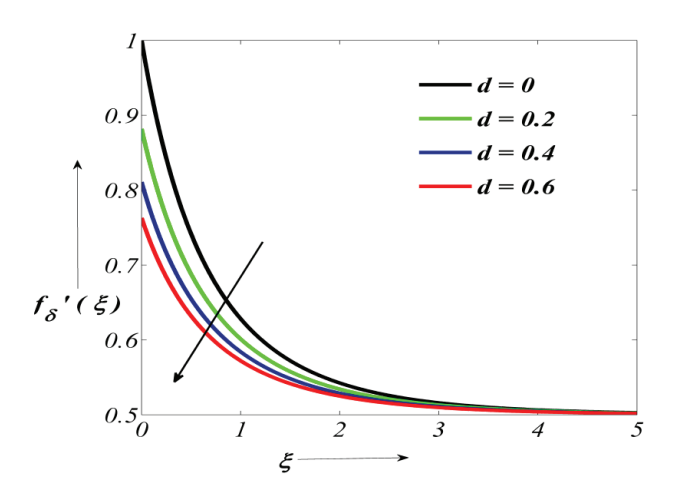


**Figure 11.** Velocity profile against *d*.

Figure 10 demonstrates that fluid concentration and concentration boundary layer thickness decline as values increase, implying more efficient mixing or dispersion. Table 5 reveals that the Nusselt number decreases while the Sherwood number increases as increases, indicating changes in convective heat transfer efficiency and mass transfer efficiency, respectively. Figure 10 illustrates the effect of d (0.0, 0.2, 0.4, 0.6) on the velocity distribution. It's noticeable that fluid velocity falls down as d rises up, as

depicted in Figure 11 and plots are distinct for  $0.0 \le \xi \le 4.0$  (approx) and follows convergence criterion for  $\xi \to \infty$ . The primary reason for this velocity reduction is the occurrence of slip conditions. Consequently, the width of the boundary layer decreases with increasing values of velocity slip parameter d.

## CONCLUSION

P.D.E's are converted into a set of O.D.E's by the use of similarity transformation on it. Final results include the velocity, temperature and concentration distribution of MHD Casson nanofluid flow and impact of outer velocity induced by stretching cylinder. Final outcomes of the study are:

- Augmentation in free stream velocity shows the increase in fluid velocity.
- The Skin friction coefficient intensifies with increment in free stream velocity parameter.
- Temperature of fluid reduced with increment of λ whereas noticed opposite pattern in case of Nb, Nt, d and Rd.
- Heat transfer rate falls down by 71.31% with increment in free stream velocity as  $0.1 \le \lambda \le 0.7$ .
- λ shows more deviation in temperature profile between fluid layer. On the other hand, *Rd* left more impact on temperature of fluid as comparative to the other parameter like *Nb*, *Nt* and *d*.
- Concentration of fluid reduced for higher  $\lambda$ , Nb and Rd and opposite trend has been seen in cases of Nt and d.
- *Nt* and *Nb* shows more deviation as comparative to other parameter in case of concentration of fluid.

Current study is limited to the incompressible laminar flow of nanofluids induced by stretching cylinder in presence of free stream velocity and thermal radiation. This analysis can be extended to three dimensional extended surface induced with Cattaneo-Christov heat flux, melting surface utilizing Lie symmetry analysis.

#### **NOMENCLATURE**

λ	Outer velocity parameter
Rd	Radiation parameter
d	Velocity slip parameter
Nt	Thermophoresis
n	Non-linear stretching parameter
L	Characteristic length
Rc	Constant
Nb	Brownian motion
$U_w$	Stretching velocity
r	Radius of cylinder
и, v	Horizontal & radial velocity
T	Temperature
C	Concentration
$T_{\infty}$	Ambient temperature

Brownian diffusion coefficient

- $D_T$ Thermophoretic diffusion coefficient
- $C_{\infty}$ Ambient concentration
- σ Electrical conductivity
- $B_0$ Magnetic field strength
- Density ρ
- Stretching velocity parameter е
- α Thermal diffusivity
- Ratio of heat capacity τ
- Velocity slip factor  $N\mu$
- Prandtl number Pr
- M Magnetic parameter
- $\theta_{\delta}$ Temperature distribution
- Velocity distribution  $f_{\delta}$
- Sc Schmidt number
- Rd Heat radiation
- $\phi_{\delta}$ Concentration distribution
- Q Heat generation
- $Sh_r$ Sherwood number
- Nusselt number  $Nu_r$
- $C_w$ Wall concentration
- Fluid temperature
- $T_f$   $C_f$ Skin friction coefficient
- k Thermal conductivity
- Dynamic viscosity
- $Re_x$ Local Reynolds number
- Curvature parameter γ
- b Constant
- $N_0$ Constant wall slip velocity

# **AUTHORSHIP CONTRIBUTIONS**

Authors equally contributed to this work.

#### **DATA AVAILABILITY STATEMENT**

The authors confirm that the data that supports the findings of this study are available within the article. Raw data that support the finding of this study are available from the corresponding author, upon reasonable request.

## **CONFLICT OF INTEREST**

The author declared no potential conflicts of interest with respect to the research, authorship, and/or publication of this article.

#### **ETHICS**

There are no ethical issues with the publication of this manuscript.

## STATEMENT ON THE USE OF ARTIFICIAL **INTELLIGENCE**

Artificial intelligence was not used in the preparation of the article

#### **REFERENCES**

- Crane LJ. Flow past a stretching plate. Zeitschrift für angewandte Mathematik und Physik ZAMP 1970;21:645-647. [Crossref]
- Yoon BB, Rao RS, Kikuchi N. Sheet stretching: a theoretical-experimental comparison. Int J Mech Sci. 1989;31:579-590. [Crossref]
- Sarma MS, Rao BN. Heat transfer in a viscoelastic fluid over a stretching sheet. J Math Anal Appl. 1998;222:268-275. [Crossref]
- Manjunatha PT, Gireesha BJ, Prasannakumara BC. [4]Effect of radiation on flow and heat transfer of MHD dusty fluid over a stretching cylinder embedded in a porous medium in presence of heat source. Int J Appl Comput Math. 2017;3:293-310. [Crossref]
- Choi SU, Eastman JA. Enhancing thermal conductivity of fluids with nanoparticles. Argonne National Lab. 1995. ANL/MSD/CP-84938; CONF-951135-29.
- Buongiorno J. Convective transport in nanofluids. J Heat Transfer 2006;128:240-250. [Crossref]
- Ahmed SE, Arafa AA, Hussein SA. Bioconvective flow of a variable properties hybrid nanofluid over a spinning disk with Arrhenius activation energy, Soret and Dufour impacts. Numer Heat Transfer A Appl 2024;85:900-22. [Crossref]
- Mebarek-Oudina F, Preeti Sabu AS, Vaidya H, Lewis [8] RW, Areekara S, et al. Hydromagnetic flow of magnetite-water nanofluid utilizing adapted Buongiorno model. Int J Mod Phys B 2024;38:2450003. [Crossref]
- Sheikholeslami M, Khalili Z. Simulation for impact of nanofluid spectral splitter on efficiency of concentrated solar photovoltaic thermal system. Sustain Cities Soc. 2024;101:105139. [Crossref]
- [10] Jayadevamurthy PGR, Rangaswamy Prasannakumara BC, Nisar KS. Emphasis on unsteady dynamics of bioconvective hybrid nanofluid flow over an upward-downward moving rotating disk. Numer Methods Part Differ Equ 2024;40:e22680. [Crossref]
- Sepehrnia M, Mohammadzadeh K, Rozbahani [11] MH, Ghiasi MJ, Amani M. Experimental study, prediction modeling, sensitivity analysis, and optimization of rheological behavior and dynamic viscosity of 5W30 engine oil based SiO2/MWCNT hybrid nanofluid. Ain Shams Eng J 2024;15:102257.
- [12] Hayat T, Asad S, Alsaedi A. Flow of Casson fluid with nanoparticles. Appl Math Mech. 2016;37:459-70.
- Siddheshwar PG, Mahabaleshwar US. Flow and [13] heat transfer to a Newtonian fluid over non-linear extrusion stretching sheet. Int J Appl Comput Math 2018;4:1-24. [Crossref]
- [14]Abbas Z, Hayat T. Stagnation slip flow and heat transfer over a nonlinear stretching sheet. Numer Methods Part Differ Equ 2011;27:302-14. [Crossref]

- [15] Dandapat BS, Chakraborty S. Effects of variable fluid properties on unsteady thin-film flow over a non-linear stretching sheet. Int J Heat Mass Transf 2010;53:5757–63.
- [16] Cortell R. Viscous flow and heat transfer over a nonlinearly stretching sheet. Appl Math Comput 2007;184:864–873. [Crossref]
- [17] Rana P, Bhargava R. Flow and heat transfer of a nanofluid over a nonlinearly stretching sheet: a numerical study. Commun Nonlinear Sci Numer Simul 2012;17:212–226. [Crossref]
- [18] Fenchouche Z, Chakir M, Benzineb O, Boucherit MS, Tadjine M. Control design for non-linear uncertain systems via coefficient diagram method: application to solar thermal cylindrical parabolic trough concentrators. Nonlinear Dyn Syst Theory 2020;20:21–37.
- [19] Tuffaha MZ, Alrefaei MH. General simplex method for fully fuzzy linear programming with the piecewise linear fuzzy number. Nonl Dyn Sys Theo 2020;20:451–460.
- [20] Khan SA, Nie Y, Ali B. Multiple slip effects on magnetohydrodynamic axisymmetric buoyant nanofluid flow above a stretching sheet with radiation and chemical reaction. Symmetry 2019;11:1171.

  [Crossref]
- [21] Akaje TW, Olajuwon BI, Musiliu Tayo RAJI. Computational analysis of the heat and mass transfer in a casson nanofluid with a variable inclined magnetic field. Sigma J Eng Nat Sci 2023;41:512–23. [Crossref]
- [22] Boların G, Yusuf A, Adekunle ST, Aıyesımı YM, Jıya M. Analysis of a boundary layer flow of a nanofluid over an inclined plane via ADM. Sigma J Eng Nat Sci 2019;37:475–88.
- [23] Gholinia M, Javadi H, Gatabi A, Khodabakhshi A, Ganji DD. Analytical study of a two-phase revolving system of nanofluid flow in the presence of a magnetic field to improve heat transfer. Sigma J Eng Nat Sci 2019;37:340–60.
- [24] Rana P, Ma J, Zhang Y, Chen J, Gupta G. Finite element and neural computations for energy system containing conductive solid body and bottom circular heaters utilizing Ag–MgO (50:50)/water hybrid nanofluid. J Magn Magn Mater 2023;577:170775.
- [25] Rana P, Ma J, Zhang Y, Gupta G. FEM simulation and optimization for thermal performance of a

- hybrid magneto-nanofluid in an inclined free convective energy system. Alex Eng J 2023;70:45–59.
- [26] Akinshilo AT, Mabood F, Ilegbusi AO. Heat generation and nonlinear radiation effects on MHD Casson nanofluids over a thin needle embedded in porous medium. Int Commun Heat Mass Transf 2021;127:105547. [Crossref]
- [27] Akinshilo AT. Thermal performance evaluation of MHD nanofluid transport through a rotating system undergoing uniform injection/suction with heat generation. Bionanoscience 2019;9:740–8. [Crossref]
- [28] Akinshilo AT, Ilegbusi A, Ali HM, Surajo AJ. Heat transfer analysis of nanofluid flow with porous medium through Jeffery Hamel diverging/converging channel. J Appl Comput Mech 2020;6:433–44.
- [29] Akinshilo AT. Mixed convective heat transfer analysis of MHD fluid flowing through an electrically conducting and non-conducting walls of a vertical micro-channel considering radiation effect. Appl Therm Eng 2019;156:506–13. [Crossref]
- [30] Makkar V, Poply V, Goyal R, Sharma N. Numerical investigation of MHD Casson nanofluid flow towards a nonlinear stretching sheet in presence of double-diffusive effects along with viscous and ohmic dissipation. J Therm Eng 2021;7:1–17. [Crossref]
- [31] Dang K, Makkar V, Sharma N. Numerical analysis of three-dimensional magnetohydrodynamics non-Newtonian free stream flow induced by permeable stretching surface. J Therm Eng 2021;10:1465–79. [Crossref]
- [32] Khan MI, Tamoor M, Hayat T, Alsaedi A. MHD boundary layer thermal slip flow by nonlinearly stretching cylinder with suction/blowing and radiation. Results Phys 2017;7:1207–11. [Crossref]
- [33] Haq RU, Nadeem S, Khan ZH, Akbar NS. Thermal radiation and slip effects on MHD stagnation point flow of nanofluid over a stretching sheet. Phys E 2015;65:17–23. [Crossref]
- [34] Reddy Gorla RS, Sidawi I. Free convection on a vertical stretching surface with suction and blowing. Appl Sci Res 1994;52:247–57. [Crossref]
- [35] Makinde OD, Aziz A. Boundary layer flow of a nanofluid past a stretching sheet with a convective boundary condition. Int J Therm Sci 2011;50:1326–32. [Crossref]